ARMY RESEARCH LABORATORY

Numerical Exploration of the Stable Boundary Layer

by Benjamin T. MacCall, Patrick A. Haines, David G. Grove, and Wen-Yih Sun

ARL-TN-323 **July 2008**

NOTICES

Disclaimers

The findings in this report are not to be construed as an official Department of the Army position unless so designated by other authorized documents.

Citation of manufacturer's or trade names does not constitute an official endorsement or approval of the use thereof.

Destroy this report when it is no longer needed. Do not return it to the originator.

Army Research Laboratory
White Sands Missile Range, NM 88002-5501

ARL-TN-323 **July 2008**

Numerical Exploration of the Stable Boundary Layer

Benjamin T. MacCall, Patrick A. Haines, and David G. Grove
Computational and Information Sciences Directorate, ARL

Wen-Yih Sun
Purdue University

REPORT DOCUMENTATION PAGE			Form Approved OMB No. 0704-0188

1. REPORT DATE *(DD-MM-YYYY)*	2. REPORT TYPE	3. DATES COVERED (From - To)
July 2008	Final	1 October 2006–30 September 2007

4. TITLE AND SUBTITLE
Numerical Exploration of the Stable Boundary Layer

5a. CONTRACT NUMBER

5b. GRANT NUMBER

5c. PROGRAM ELEMENT NUMBER

6. AUTHOR(S)
Benjamin T. MacCall, Patrick A. Haines, David G. Grove, and Wen-Yih Sun*

5d. PROJECT NUMBER
DRI FY07

5e. TASK NUMBER

5f. WORK UNIT NUMBER

7. PERFORMING ORGANIZATION NAME(S) AND ADDRESS(ES)
U.S. Army Research Laboratory
ATTN: AMSRD-ARL-CI-EM
White Sands Missile Range, NM 88002-5501

8. PERFORMING ORGANIZATION REPORT NUMBER
ARL-TN-323

9. SPONSORING/MONITORING AGENCY NAME(S) AND ADDRESS(ES)

10. SPONSOR/MONITOR'S ACRONYM(S)

11. SPONSOR/MONITOR'S REPORT NUMBER(S)

12. DISTRIBUTION/AVAILABILITY STATEMENT
Approved for public release; distribution is unlimited.

13. SUPPLEMENTARY NOTES
*Purdue University, Dept. of Earth & Atmospheric Science, West Lafayette, IN 47907

14. ABSTRACT

The planetary boundary layer under strong, stable stratification continues to elude quantitative description despite its relatively frequent occurrence and many years of effort. Measurements indicate that stable boundary layers (SBLs) possess complex temperature and wind structures which apparently provide favorable conditions for the development of the many interacting processes that can occur within the SBL. Consequently, SBLs are subject to sporadic overturning and turbulent episodes. The National Taiwan University/Purdue University nonhydrostatic model has been outfitted with a Reynolds stress turbulence closure scheme to provide a numerical test bed for probing these environments. The model has been efficiently parallelized for the U.S. Army Research Laboratory Major Shared Research Center advanced technology clusters, enabling runs utilizing 960 processors while only losing about 10% to communication overhead. The value of the new closure scheme can be seen when simulating the phenomenon of shear instability in a stably stratified layer. The new model shows several features that are more difficult to recreate in the previous turbulence scheme, such as rapid amplification of unstable modes and Kelvin-Helmholtz billows. Given the promise of the new model, future work has begun in more realistic conditions.

15. SUBJECT TERMS
turbulence, numerical modeling, stable boundary layer

16. SECURITY CLASSIFICATION OF:			17. LIMITATION OF ABSTRACT	18. NUMBER OF PAGES	19a. NAME OF RESPONSIBLE PERSON
a. REPORT	b. ABSTRACT	c. THIS PAGE			Benjamin T. MacCall
UNCLASSIFIED	UNCLASSIFIED	UNCLASSIFIED	UL	20	19b. TELEPHONE NUMBER (*Include area code*) (575) 678-6528

Standard Form 298 (Rev. 8/98)
Prescribed by ANSI Std. Z39.18

Contents

List of Figures

Acknowledgments

This work was performed while Ben MacCall held a National Research Council Research Associateship Award at the U.S. Army Research Laboratory (ARL), White Sands Missile Range, NM. The authors gratefully acknowledge use of the high performance computing facilities at the ARL Major Shared Resource Center at Aberdeen Proving Ground, MD, and support as a Department of Defense Challenge Project.

INTENTIONALLY LEFT BLANK.

1. Objective

Better understanding the stable boundary layer (SBL) through high-resolution numerical modeling is the goal of this report. At all phases, the model results are compared to analytical results and actual observations. The numerical computations should reveal SBL details, requiring further experimental verification and model enhancements.

2. Approach

Currently, SBL processes are simulated to provide a virtual laboratory to develop quantitative predictions on the role of various processes commonly observed in stable environments. Specific focus is on how gravity waves, generated by shear and terrain, may alter the state of localized regions within the SBL, thus allowing turbulence to develop. Simulation results are being carefully compared with current observational data, other numerical treatments, and laboratory experiments to refine modeled terms. Successful simulation should stimulate new experimental efforts in verification and model refinement. Contrary to general perception, temperature and wind profiles drawn through relatively coarse resolution observations may belie the presence of small-scale structures as seen in the acoustic sounder observations in figure 1.

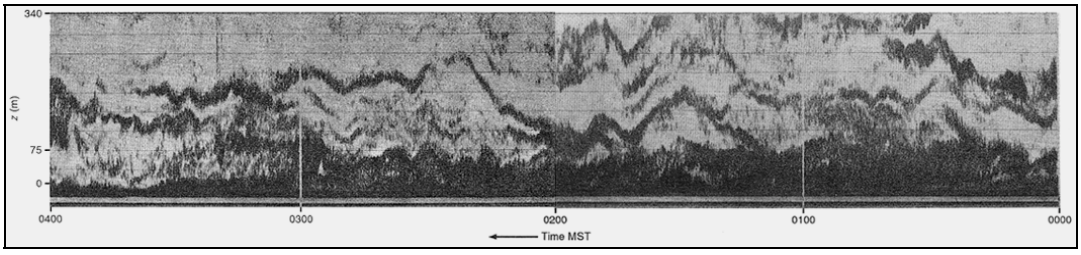

Figure 1. Acoustic sounder profiles showing turbulent activity deformed gravity waves (*1*).

Observations have shown sublayers where temperature and wind gradients are more favorable for instability (figure 2). These layers are then deformed by mesoscale motions propagating through the SBL (*2*). How these features form is poorly understood, but gravity waves (ubiquitous in the SBL) may be one responsible mechanism. During the month-long CASES-99 experiment, wave activity was observed nightly (*3*). Gravity waves transporting momentum and energy without loss is well documented (*2*, *4*, *5*). What is investigated here is whether gravity waves, created internally or externally to the SBL, can alter the state of small regions within the boundary layer, fostering instability. The resulting turbulence becomes part of a complicated system of energy and momentum exchange between the turbulence, waves, and mean flow.

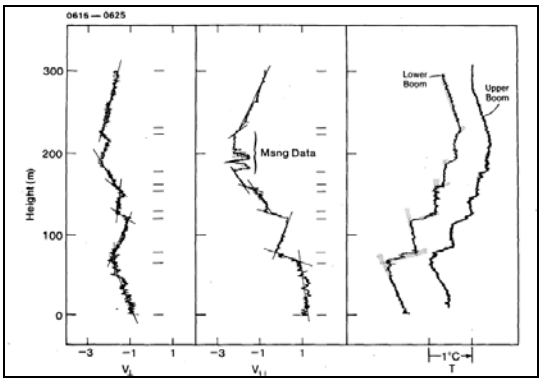

Source: Boulder Atmospheric Observatory.

Figure 2. Observations using a translatable boom with meteorological instruments (*2*).

If the energy and momentum transfer is between the SBL and free atmosphere, universal scaling will not be very accurate (*6*).

Current efforts center on describing the fine-structure evolution instead of improving bulk SBL parameterizations. Initial focus is on the shear instability and terrain effects that produce gravity waves. To explore wave-turbulence interactions, the model must resolve small-scale structures yet properly generate and trap gravity waves. Mechanisms for the ducting of gravity waves include critical levels (*5*), Doppler ducting (*7*), and thermal ducting (if the SBL is bounded by neutral or convective lapse rates). The National Taiwan University/Purdue University (NTU/PU) nonhydrostatic model (*8, 9*), modified to include a more complete treatment of turbulence in stably stratified environments, was used. The model has been developed for more than 10 years and applied to several different physical situations, such as nonlinear mountain waves, shallow convection due to cold-air outbreaks, deep-vortex generation, and shedding.

The NTU/PU model uses the prognostic equation for density instead of a pressure tendency equation. The method also explicitly resolves acoustic waves without time filtering. Due to the small time step required to satisfy the Courant-Friedrichs-Lewy criterion for acoustic waves, two methods are used to conserve computational resources. By decreasing the speed of sound, the largest stable time interval can be increased without affecting the meteorological evolution. Also, the model uses a split time step integration scheme to update slower varying physics in a more appropriate interval. Finally, by avoiding the difficulties of solving pressure tendency equations, the model is more easily parallelized for efficient use of massively parallel clusters (*8*) and uses a stretchable (in all three directions) terrain-following grid. Using a nested high-resolution region allows more complicated lateral and upper boundary conditions to be specified, which is especially important when simulating conditions to prevent gravity waves from propagating out of the system. The terrain-following vertical coordinate (σ-z) is prescribed at model initialization to include terrain effects.

In environments with strong stratification, turbulent motions are damped in the vertical direction leading to anisotropy of the turbulent field (*10*). In an eddy-viscosity closure scheme, flow history takes a reduced role; fluctuations are mostly dependent on the instantaneous mean strain rates. Isotropic flow history only enters through the variables used to calculate eddy viscosity and eddy diffusivity, usually by turbulent kinetic energy (TKE) and dissipation. NTU/PU's default turbulence scheme model is a single equation eddy-viscosity scheme. TKE is solved prognostically while the length scale is prescribed and is based on model grid spacing and stratification. It is now computationally feasible to prognostically calculate transport equations for turbulent moments (a method developed in the 70s by several groups). The method employed in the NTU/PU model was developed by Lumley (*11–13*). Several terms of the second-order equations can be calculated explicitly. Some of the other terms—deviatoric dissipation, isotropic pressure dissipation, and molecular diffusion—are neglected. Deviatoric pressure dissipation is modeled using a return-to-isotropy and rapid strain with buoyancy contributions. The second-order model equations are as follows:

the TKE:

$$\partial_t e + U_\ell \partial_\ell e = -\overline{u'_\ell u'_i} S_{i\ell} - \frac{1}{2} T^{(e)} + \frac{g}{\theta_o} \overline{u'_3 \theta'} - \varepsilon \,; \tag{1}$$

the potential temperature variance:

$$\partial_t \overline{\theta'^2} + U_\ell \partial_\ell \overline{\theta'^2} = -\overline{u'_\ell \theta'} \partial_\ell \Theta - \frac{1}{2} T^{(\theta)} - 2\varepsilon_\theta \,; \tag{2}$$

the heat flux:

$$\partial_t \overline{u'_j \theta'} + U_\ell \partial_\ell \overline{u'_j \theta'} = -\frac{2}{5} \overline{u'_\ell \theta'} S_{\ell j} - \left(b_{\ell j} + \frac{2}{3} e \delta_{\ell j} \right) - T_j^{(\theta)} - \frac{C_\theta}{\tau_\varepsilon} \overline{u'_j \theta'} + \frac{2}{3} \delta_{j3} \frac{g}{\theta_0} \overline{\theta'^2} \,; \tag{3}$$

and the deviatoric momentum flux:

$$\partial_t b_{ij} + U_\ell \partial_\ell b_{ij} = -\frac{8}{15} e S_{ij} - \frac{1}{5} \Sigma_{ij} - R_{ij} - T_{ij}^{(b)} - \frac{C_b}{\tau_\varepsilon} b_{ij} + \frac{13}{10} B_{ij} \,; \tag{4}$$

where

$$S_{i\ell} = \frac{1}{2}\left(\partial_\ell U_i + \partial_i U_\ell\right),\ R_{i\ell} = \frac{1}{2}\left(\partial_\ell U_i - \partial_i U_\ell\right),\ T^{(e)} = \frac{1}{2} \partial_j \overline{u'_\ell u'_i u'_j},\ T^{(\theta)} = \partial_j \overline{u'_j \theta'^2},$$

$$b_{ij} = \overline{u'_i u'_j} - \frac{2}{3} e \delta_{ij},\ C_b = \frac{1}{15 II}\left(1 + \sqrt{1 + 24 II}\right),\ C_\theta = \frac{C_{\varepsilon\theta}}{C_\varepsilon} + \frac{C_b}{2}, \text{ and } II = \frac{1}{2} b_{ij} b_{ij}. \tag{5}$$

This method is augmented by the dissipation spectra for stable stratification developed by Canuto and Minotti (*10*). For coarse resolution simulations under strong stratification, a volume element is too large to resolve isotropic turbulent fluctuations. Applying the Kolmogorov

similarity for the inertial subrange overestimates the amount of energy cascading to smaller scales; the subgrid turbulent motions work against the stratification, leaving less to cascade. As grid spacing becomes much smaller than the buoyancy length scale ($\Delta_b = \sqrt{e}/N$), unresolved motions become isotropic and dissipation again follows the Kolmogorov spectrum. The functional form of the dissipation is as follows:

$$\varepsilon = C_\varepsilon(e)\frac{e^{3/2}}{\Delta}\ , \tag{6}$$

and

$$\varepsilon = C_{\varepsilon\theta}(e)\overline{\theta'^2}\frac{e^{1/2}}{\Delta}, \tag{7}$$

with dissipation coefficients,

$$C_\varepsilon(e) = c_\varepsilon \exp\left[-0.053\frac{N^2\Delta^2}{e}\right] \text{ and } C_{\varepsilon\theta}(e) = C_\varepsilon\left[\frac{c_\theta}{c_\varepsilon} - 2\gamma(\omega - 1)\frac{e}{\overline{\theta'^2}}\right], \tag{8}$$

where

$$c_\varepsilon = \pi\left(\frac{2}{3Ko}\right)^{3/2},\ c_\theta = \frac{4\pi}{3Ba}\left(\frac{2}{3Ko}\right)^{1/2},\ \omega(e) = \exp\left(-0.053\frac{N^2\Delta^2}{e}\right),$$

$$\gamma = \frac{|\nabla T|^2}{N^2}, \text{ and } \Delta = \min(\Delta x, \Delta y, \Delta z). \tag{9}$$

The derivation of the second-order transport equations does not introduce any new information into the equation system; previously implicit forcing is simply exposed. As such, closure is not introduced due to the presence of the third-order moments, the turbulent transport terms. A similar process yields third-order transport equations. To introduce closure, a quasi-Gaussian assumption is employed to rewrite the fourth-order moments as a function of the second-order moments (*11*). Over the bulk of the SBL, these terms should have a small effect; however, in regions of instability, the third-order terms may possibly influence the evolution of the small-scale structures. Due to the computational requirements for prognostically solving such equations, preliminary simulations have completely neglected third-order correlations. However, given the recently completed parallel version of the turbulence closure module, third-order equations can now be practically integrated.

Although initial feasibility testing of the three-dimensional higher-order closure model (*14*) was done in the serial version of the NTU/PU model, sensitivity testing and probing was not practical given the serial model's limited resources. The new closure module has been rewritten to employ the message-passing interface (MPI) libraries for parallel execution and has been added to the parallel version of the NTU/PU model. The parallel version enables the large

computational domains and high resolutions required to capture the larger and smaller scale processes observed in the SBL. So far, the performance numbers are favorable and should not hinder future large simulations. An example is a domain with 1200 × 150 horizontal grid points and 60 vertical levels. Figure 3a shows the performance gained by increasing the number of processors leaving the domain size constant.

The better-than-double performance is likely attributed to better processor cache usage with smaller domains and smaller amounts of data copied in the custom variable packing routines. Of course, for increasing number of processors, CPU resources are offset by an increase in communication overhead, thus reducing performance. Since our focus is on running high-resolution, large-domain simulations, a more relevant comparison is to test scalability by choosing a reasonable subdomain for each processor. Therefore, as a greater number of processors are used, the domain increases. This prevents the total domain from being divided into pieces too small to be efficient as the number of processors becomes large. Hence, the domain on each processor was held at 30 × 25 horizontal grid points with 60 vertical levels. Ideally, as the number of processors increases, the computational time should remain constant; however, the overhead needed for parallel communication prevents the ideal case. As figure 3b shows, employing 960 processors leads to an 11% decrease in efficiency, neglecting output. The final simulation domain was 1200 × 600 × 60 grid points. Data input/output (I/O) also required careful consideration. I/O was treated using the Hierarchical Data Format v5 (HDF5) libraries developed at the University of Illinois National Center for Supercomputing Applications. HDF5 is an abstracted I/O library that can create structured, self-describing, random-access files using independent and collective (parallel) I/O operations.

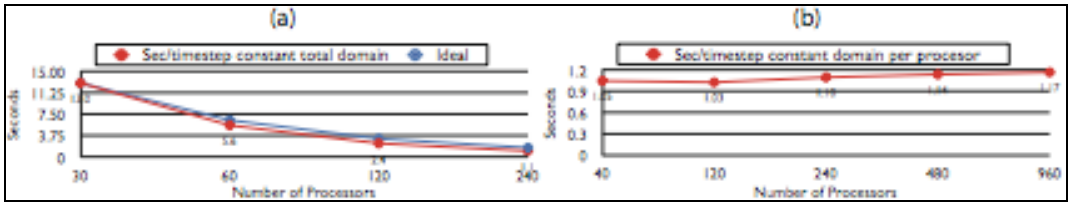

Figure 3. Input performance results for (a) constant total domain split over an increasing number of processors and (b) a domain that increases proportional to the number of processors.

3. Results

The initial simulations used a serial model version (*14*); extensive testing of the closure module was impractical. More testing is needed to confirm that the results are physical and not caused by numerical issues (e.g., contamination by lateral boundary conditions). Kelvin-Helmhotz (KH) instability is the dominant SBL turbulence mechanism; it results from wind shear present from the bottom of the free atmosphere extending into the boundary. Thin layers of relatively strong shear may develop as gravity waves dump momentum into localized regions; thus,

properly simulating shear instability is a primary concern. The simulations were initialized with a 100-m-deep shear layer in the middle of the domain, with a 4.9 m/s velocity difference. The shear region velocity profile was defined by a hyperbolic tangent function; the thermal gradient was defined by a constant Brunt-Vaisala frequency. A random perturbation was added to the initial u-wind field. Using the single-equation eddy-viscosity closure scheme, the turbulent diffusion smoothes the perturbations, preventing amplification of the preferred mode and resulting in TKE profiles (figure 4a and b).

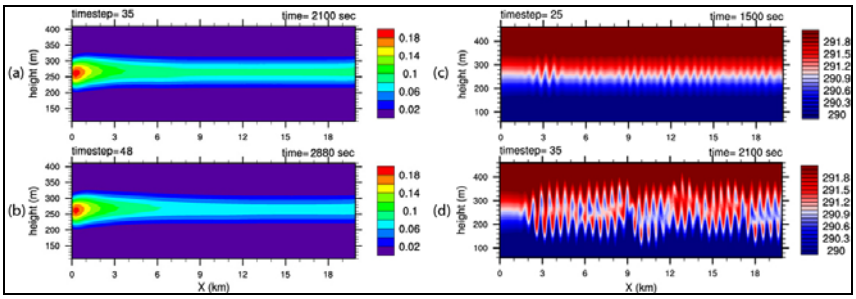

Figure 4. TKE profiles simulated using an eddy-viscosity closure for (a) 35 and (b) 48 min. Potential temperature (to show overturning) using second-order closure for (c) 25 and (d) 35 min.

Switching to a second-order closure reveals a different evolution (figure 4c and d). By 25 min into the simulation, a narrow band of modes is clearly present. By 35 min, the waves are breaking, forming KH billows. A spectral decomposition shows the energy distribution during the wave growth and breaking phases (figure 5). Linear theory predicts the amplification of a single preferred mode proportional to the shear layer depth (the red line on the spectral plots) (*15*). In the initial wave growth, a narrow band of modes surrounding the linear mode is stimulated. Later, during wave breaking, the linear mode is still dominant, but secondary modes also appear, especially at lower wave numbers, which have been observed in nature (figure 6). Breaking waves are the primary instability associated with shear; however, several other effects have been observed: subharmonic vortex pairing, convective rolls development with vorticity perpendicular to the vorticity of the billow, vortex knotting, and vortex tube formation (*16*). With the new MPI model, simulating such effects to support the model's ability to accurately treat subtle processes will be attempted.

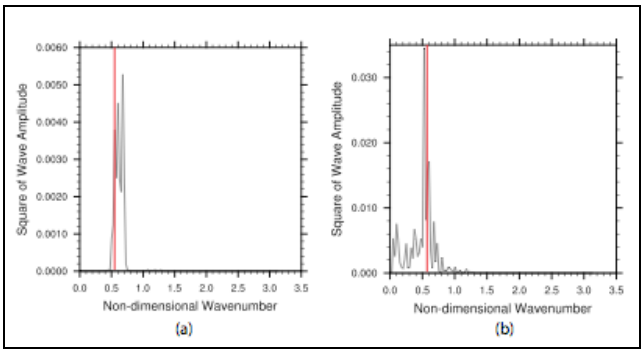

Figure 5. Fourier modes: (a) 25 min during initial wave excitation and (b) 35 min during wave breaking.

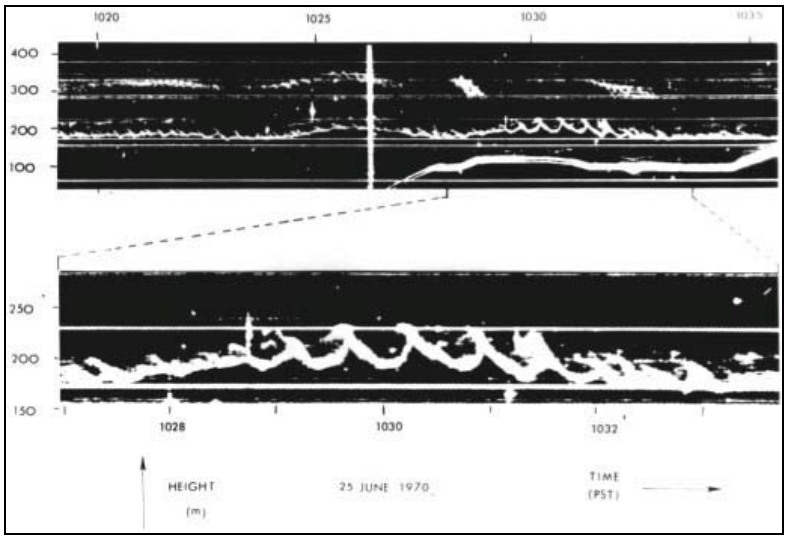

Figure 6. Frequency modulated continuous wave radar image of KH waves showing the presence of two separate modes (*2*).

4. Conclusions

The SBL continues to elude quantitative description; much work remains for theorists, experimentalists, and modelers. Given the observed fine-scale structures, numerical modeling may provide a cost-effective way of probing the behavior. The overall goal of this project is to simulate this complicated behavior. The interactions between fine-scale turbulence, larger-scale features provided the impetus for implementing a new higher-order turbulence closure routine into the NTU/PU model. Preliminary results from the series version of the code were encouraging, but the inability to take advantage of massively parallel clusters significantly limited the scope of testing. An efficient parallel version of the model code has been developed. Using the U.S. Army Research Laboratory HPC clusters, expanded simulations of shear

instability supported the utility of the new scheme. The model showed rapid amplification of perturbations in a narrow band of preferred nodes in agreement with linear theory. The amplification led to the development of wave breaking, Kelvin-Helmholtz billows and the eventual decay of the turbulence. Because shear instability is the primary source of turbulence in the SBL and the most common mechanism for the production of gravity waves, accurate simulation of shear instability will play an important role in probing gravity wave-turbulence interactions.

Much work remains to be done, and more comprehensive simulations are being planned. An important goal is to demonstrate the destabilization of thin sublayers embedded within the SBL via in-bound gravity waves. The effects of nonuniform terrain and terrain-generated gravity waves will also be included. Later in 2008, more holistic runs will be attempted by initializing the model with observations from CASES-99 field experiments. These model runs will provide an important test of the utility of the model in more realistic environments and will hopefully produce quantitative, testable predictions that will facilitate new theoretical work on transient turbulence, turbulence under stable conditions, and new field experiments. Ultimately, we hope to contribute to better forecasts of meteorological conditions at night, when the Army prefers to operate, and the dispersion and diffusion of chemical, biological, or radiological agents.

5. References

1. Nappo, C. J. *Intro. to Atmos*. *Gravity Waves*; Inter. Geophysics Series; Academic Press: New York, 2002.
2. Chimonas, G. Steps, Waves and Turbulence in the Stably Stratified Planetary Boundary Layer. *Bound. Layer Met*. **1999**, *90*, 397–421.
3. Chimonas, G. On Internal Gravity Waves Associated With the Stable Boundary Layer. *Bound. Layer Met.* **2002**, *102*, 139–155.
4. Lindzen, R. S.; Holton, J. R. *A Theory of the Quasi-Biennial Oscillation* **1968**, *25*, 1095–1107.
5. Booker, J. R.; Bretherton, F. P. The Critical Layer for Internal Gravity Waves in a Shear Flow. *J. Fluid Mech.* **1967**, *27*, 513–519.
6. Finnigan, F. A Note on Wave-Turbulence Interaction and the Possibility of Scaling the Very Stable Boundary Layer. *Bound. Layer Met.* **1999**, *90*, 529–539.
7. Chimonas, G.; Hines, C. O. Doppler Ducting of Atmospheric Gravity Waves. *J. Geophys. Res.* **1986**, *91* (D1), 1219–1230.
8. Hsu, W.-R.; Sun, W.-Y. A Time-Split, Forward-Backward Numerical Model for Solving a Nonhydrostatic and Compressible System of Equations. *TELLUS* **2001**, *53A*, 279–299.
9. Hsu, W.-R.; Sun, W.-Y.; Tcheng, S.-C.; Chang, H.-Y. Parallelization of the NTU-Purdue Non-Hydrostatic Numerical Model: Simulation of the 11 January 1972 Boulder Windstorm. *Proceedings of the 7th National Computational Fluid Dynamics Conference*, Kenting, 2000.
10. Canuto, V. M.; Minotti, F. Stratified Turbulence in the Atmosphere and Oceans: A New Subgrid Model. *J. Atmos. Sci.* **1993**, *50* (13), 1925–1935.
11. Lumley, J. L. Modeling Turbulent Flux of Passive Scalar Quantities in Inhomogeneous Flows. *Physics of Fluids* **1975**, *18*, 619–621.
12. Lumley, J. L. Computational Modeling of Turbulent Flows. *Adv. App. Mech*. **1978**, *18*, 123–176.
13. Lumley, J. L. Second Order Modeling of Turbulent Flows. In *Von Karman Institute Lecture Series*, No. 2; Rhode Saint Genese Belgium, 1979.
14. MacCall, B. Application of Reynolds' Stress Closure to SBLs. Ph.D. Thesis, Purdue University, IN, 2006.

15. Scinocca, J. F. The Mixing of Mass and Momentum By Kelvin-Helmholtz Billows. *J. Atmos. Sci*. **1995**, *52* (14), 2509–2530.

16. Thorpe, S. A. Transitional Phenomena and the Development of Turbulence in Stratified Fluids: A Review. *J. Geophys. Res.* **1987**, *92* (C5), 5231–5248.

NO. OF COPIES	ORGANIZATION
1 (PDF ONLY)	DEFENSE TECHNICAL INFORMATION CTR DTIC OCA 8725 JOHN J KINGMAN RD STE 0944 FORT BELVOIR VA 22060-6218
1	US ARMY RSRCH DEV & ENGRG CMD SYSTEMS OF SYSTEMS INTEGRATION AMSRD SS T 6000 6TH ST STE 100 FORT BELVOIR VA 22060-5608
1	DIRECTOR US ARMY RESEARCH LAB IMNE ALC IMS 2800 POWDER MILL RD ADELPHI MD 20783-1197
1	DIRECTOR US ARMY RESEARCH LAB AMSRD ARL CI OK TL 2800 POWDER MILL RD ADELPHI MD 20783-1197
1	DIRECTOR US ARMY RESEARCH LAB AMSRD ARL CI OK T 2800 POWDER MILL RD ADELPHI MD 20783-1197
	ABERDEEN PROVING GROUND
1	DIR USARL AMSRD ARL CI OK TP (BLDG 4600)

NO. OF
COPIES ORGANIZATION

1 US ARMY RESEARCH OFFICE
AMSRD ARL RO EV
W BACH
PO BOX 12211
RESEARCH TRIANGLE PARK NC
27709-2211

1 US ARMY RESEARCH LAB
AMSRD ARL CI ED
D GARVEY
2800 POWDER MILL RD
ADELPHI MD 20783-1197

1 US ARMY RESEARCH LAB
AMSRD ARL CI E
P CLARK
2800 POWDER MILL RD
ADELPHI MD 20783-1197

1 US ARMY RESEARCH LAB
AMSRD ARL CI EM
D KNAPP
BLDG 1622 RM 112A
1622 HEADQUARTERS AVE
WHITE SANDS MISSILE RANGE NM
88002-5501

1 US ARMY RESEARCH LAB
AMSRD ARL CI ED
E MEASURE
BLDG 1622 RM 205
1622 HEADQUARTERS AVE
WHITE SANDS MISSILE RANGE NM
88002-5501

1 US ARMY RESEARCH LAB
AMSRD ARL CI ED
S A LUCES
BLDG 1622 RM 201
1622 HEADQUARTERS AVE
WHITE SANDS MISSILE RANGE NM
88002-5501